ELSEVIER

Ceramics International 27 (2001) 537–541

CERAMICS INTERNATIONAL

www.elsevier.com/locate/ceramint

Influence of MgO on microstructure and properties of mullite–Mo composites fabricated by pulse electric current sintering

R. Sivakumar *, D. Doni Jayaseelan, T. Nishikawa, S. Honda, H. Awaji

Nagoya Institute of Technology, Gokiso-cho, Showa-ku, Nagoya 466 8555, Japan

Received 11 September 2000; received in revised form 19 September 2000; accepted 23 October 2000

Abstract

Mullite–Mo (10 vol.%) composites and monolithic mullite were fabricated using a pulse electric current sintering technique. Both monolith and composites of mullite were sintered up to theoretical density at 1500°C within few minutes. MgO of 0.25 wt.% was added as a sintering aid to both the mullite and composites. Addition of MgO significantly increased the bending strength of the monolithic mullite and mullite/10 vol.% Mo composites to 441 and 634 MPa respectively. The apparent increase in the bending strength of the composites was attributed to the combinational effect of Mo and MgO present in the composites. The fracture toughness of the composites also increased from 2 to 3.9 MPa.$m^{0.5}$ for the mullite/10 vol.% Mo composites, which was nearly twice that of the mullite. Crack-bridging and frontal process-zone elongation were expected to be the toughening mechanisms operated in these composites. The addition of Mo having high thermal diffusivity slightly increased the thermal diffusivity of the composites, because the 10 vol.% Mo particles were well dispersed and discontinuous in the matrix. Elongated mullite grains were observed for the composites without MgO, whereas the composites with MgO have a controlled microstructure.

Keywords: A. Sintering; B. Composites; C. Strength; C. Toughness and toughening; D. Mullite; Mo; Pulse electric current sintering (PECS)

1. Introduction

Although structural ceramics have ionic and/or covalent bonding and exhibit high bonding strength and chemical stability, fracture toughness of ceramics is quite low because of the poor plasticity. Among many researchers who have made contributions to developments of toughening ceramics such as ceramics reinforced by ductile metal dispersions, Niihara [1] developed a new concept of ceramic-based nanocomposites and showed a drastic improvement of toughness and strength of ceramics. The microstructure of the nanocomposites was composed of second-phase nano-size particles dispersed within the matrix grains. Thermal expansion mismatch between the matrix and the second-phase particles produced the significant improvement of the fracture strength by additional annealing, which was due to the further development of sub-grain boundaries around the second phase particles.

Recently Awaji et al. [2] classified the toughening mechanisms in ceramic matrix composites (CMCs) based on Griffith's energy equilibrium into three groups. (A) The frontal process-zone toughening mechanism, which is related to the intrinsic fracture energy of a material and creates a damaged zone ahead of a crack tip. The toughening in nanocomposites proposed by Niihara is mainly based on this mechanism where the intrinsic fracture energy rate increases in the energy equilibrium equation. (B) The crack-bridging toughening mechanism, which operates in a process-zone wake in a material. This mechanism produces an extrinsic increase in crack resistance after a certain extension from the initial crack length, which is caused by reduction of the stress concentration at the crack tip by the shielding. The toughening of CMCs composed of micro and macroscopic heterogeneous particles [3,4], whiskers [5] and platelets [6] is related to this mechanism. (C) The micro and macroscopic crack-deflection mechanism, where the crack is forced to deflect at the crack tip. The deflection decreases the energy-release rate in the energy equilibrium equation and consequently increases the critical stress-intensity factor at the crack tip. Toughening mechanisms of materials with multi-layered

* Corresponding author. Tel.: +81-52-735-5287; fax: +81-52-735-5294.

E-mail address: sivachi@mse.nitech.ac.jp (R. Sivakumar).

0272-8842/01/$20.00
PII: S0272-8842(00)00115-2

structures such as combinations of tough/weak materials [7–10], dense/porous materials [11,12] and structure controlled self-reinforced composites [13] belong to this group.

In this regard, new ceramic/metal composites were successfully developed [14,15]. Molybdenum (Mo) reinforced mullite matrix composites have a unique advantage of similar thermal expansion coefficients at room temperature (4.8×10^{-6} C^{-1} for mullite and 4.9×10^{-6} C^{-1} for Mo at 25°C). Because the residual stresses due to thermal expansion mismatch are expected to be small, the mullite–Mo system is used effectively in FGMs with ceramics [16,17]. MgO was added in smaller composition (0.25 wt.%) as a sintering aid for better densification.

A pulse electric current sintering (PECS) technique was used as the sintering method for consolidating the mullite–Mo composites. This sintering method is applicable to sintering poor sinterable materials at low temperature within a short time. The aim of this work is to study the influence of MgO on mechanical and thermal properties of the mullite/10 vol.% Mo composites, where the notations of 1090 and 1090N represent 10 vol.% Mo composites with and without the addition of MgO, respectively.

2. Experimental procedure

2.1. Powder preparation

Mullite powder (Kyoritsu Yogyo Co., KM102) of average particle size of 1.3 μm and molybdenum powder (Mitsuwa's Pure Chemical Co.) of average particle size of 2.7 μm were used as the starting materials to synthesis the mullite–Mo composites. MgO (Hayashi Pure Chemicals Ltd.) was added as the sintering aid to the monolithic mullite and 1090 composite specimens. These powders were well mixed in a polyethylene pot for 24 h taking uniform sized alumina balls as milling media in ethanol. This milled mixture was allowed to dry at 110°C for 24 h. Then, the mixture was ground with a high purity alumina mortar and sieved to pass through a screen of 350 μm in size.

2.2. Sintering

Mo gets easily oxidized in the air atmosphere at high temperatures. Also, the evaporation rate of Mo due to oxidation is high having exothermic reaction and it is very difficult to sinter mullite–Mo composites in normal atmospheric conditions [15]. Hence, the PECS technique was carried out in a vacuum of 4.5×10^{-5} Torr using the apparatus SPS-515S (Sumitomo Coal Mining Co., Ltd., Japan). The mixed and sieved powder was well packed in a graphite die with the outer and inner of 40 and 20 mm in diameter, respectively, with a pair of graphite punches on both sides, and was placed inside a vacuum chamber. The pressure of about 20 MPa was applied during the sintering process. The temperature could reach 1500°C in 10 min from room temperature. At the maximum temperature, specimens were held for 10 min until they showed no shrinkage and then reduced to room temperature. The sintered specimens were about 20 mm in diameter and 10 mm in height.

2.3. Characterization

The sintered density of the specimens was measured by means of Archimedes method in water medium. Young's modulus measurement was carried out using an ultrasonic method. Test bars ($2\times2\times10$ mm^3) for a flexural strength test were sliced from the sintered specimens and polished with diamond paste. A three-point bending test was carried out with the cross-head speed of 0.1 mm/min and the lower span of 8 mm. The fracture toughness was determined using an indentation fracture (IF) method by applying a load of 196 N for 15 s. The microstructure of the polished and fractured surfaces of the sintered specimens was observed by scanning electron microscopy (SEM). Thermal properties of the mullite and mullite–Mo composites were evaluated for the cylindrical discs with 10 mm in diameter and 1 mm in thickness by means of a laser flash technique. The thermal conductivity was calculated from values of specific heat, density, and thermal diffusivity of each sample.

3. Results and discussion

3.1. Density and densification curves

The relative densities of sintered specimens are shown in Table 1. The specimens were sintered using the PECS technique at 1500°C for the monolithic mullite and mullite–Mo composites. These materials have more than 97% of theoretical density.

Fig. 1 shows the shrinkage curves of the monolithic mullite, 1090 and 1090 N composite specimens. The densification started around 1050°C for all the specimens. MgO promotes sintering and densification rate for the monolithic mullite and 1090 composite with MgO, compared with the 1090 N composite without MgO addition. Since MgO is dissolved at higher temperature to promote the sintering, it is not detected in the microstructures [18]. Sintering at high temperature of the 1090 N composite without MgO showed elongated grains of mullite but the grain sizes are small, as shown in Fig. 2(a).

Table 1
Mechanical properties of mullite–Mo composites sintered by pulse electric current sintering

	Relative density (%)	Total porosity (%)	Vicker's hardness (GPa)	Young's modulus (GPa)	Bending strength (MPa)	Fracture toughness ($MPam^{0.5}$)
1090 N	97.1	2.9	10±0.5	204	438±139	3.1±1.0
1090	99.0	1.0	11±0.25	228	634±43	3.9±0.5
Mullite	98.3	1.7	13±0.5	222	441±34	2.0±0.75

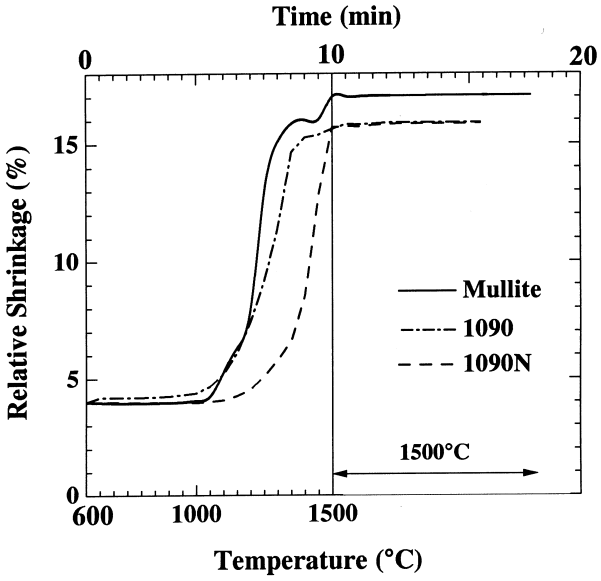

Fig. 1. Shrinkage curves of PECS treated specimens.

3.2. Microstructures

The micrographs of polished and thermally etched surfaces, and fracture surfaces of the 1090 N, 1090 composites and monolithic mullite are shown in Figs. 2 and 3 respectively. Thermal etching was carried out at 1450°C for 30 min in air atmosphere. Elongated grains of mullite are observed in the 1090 N composite as shown in the Fig. 2(a). This preferential grain growth of mullite grains in the 1090 N composites is due to sintering without addition of MgO. The microstructure of the 1090 composite is shown in Fig. 2(b). The addition of MgO influences the uniform dispersion of Mo grains in mullite matrix without forming any agglomeration. Also, the microstructure could be controlled due to pinning effect [19,20] of secondary phase Mo particles which are present on the crack surface. Fig. 2(c) shows the micrograph of thermally etched monolithic mullite. The mullite grains showed complete absence of elongated morphology due to presence of MgO. The average grain size of mullite is 2 μm.

Regarding the fracture modes of the monolithic mullite and mullite–Mo composites, the monolithic mullite indicates a mixture of intergranular and transgranular

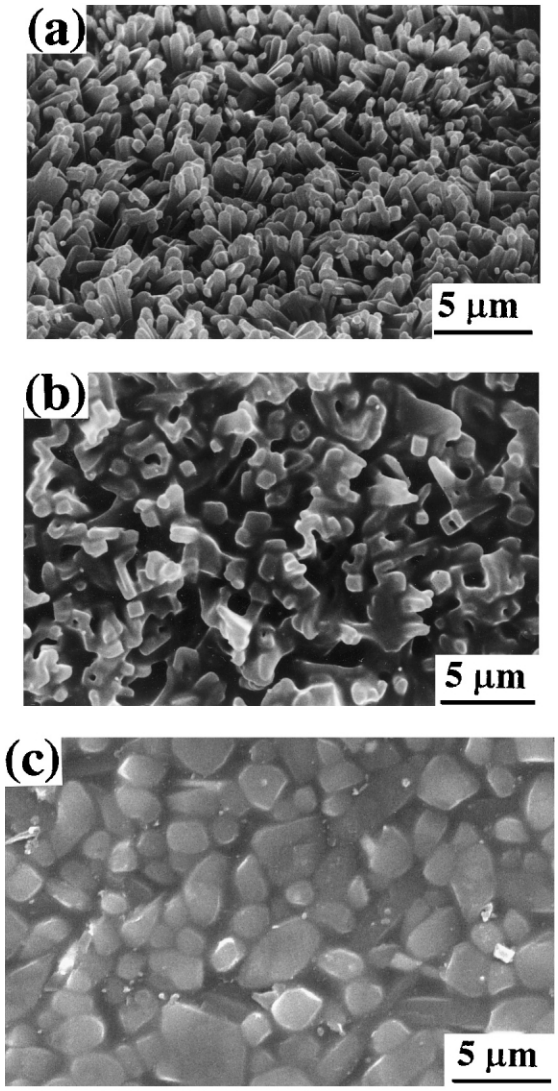

Fig. 2. Thermally etched surfaces of PECS sintered specimens. (a) 1090 N composite, (b) 1090 composite and (c) mullite.

fracture as shown in Fig. 3(c). On the other hand, the mullite–Mo composites indicate transgranular fracture mode predominantly, except for the grain boundaries of Mo as shown in Fig. 3(a) and (b). The change in the fracture mode is a result of grain boundary strengthening of the mullite due to reduction of residual stresses on the interfaces. On the cooling of monolithic mullite, residual stresses may generate on the interface caused by

the anisotropic thermal expansions according to the crystal axes. However, isotropic and ductile Mo particles, which are located in between mullite grains or dispersed inside the mullite grains may release the residual stresses on the interfaces of mullite grains.

3.3. Mechanical properties

The mechanical properties of the mullite–Mo composites and mullite fabricated by means of the PECS technique are given in Table 1. The hardness of the composites is lower than the mullite due to the addition of ductile molybdenum particles. The decrease in the Young's modulus of the 1090 N composites may be attributed to the decrease in density, inspite of the Young's modulus of Mo is higher than that of the mullite. The porosity of the 1090 composites is about a third of the 1090 N composite's porosity (Table 1).

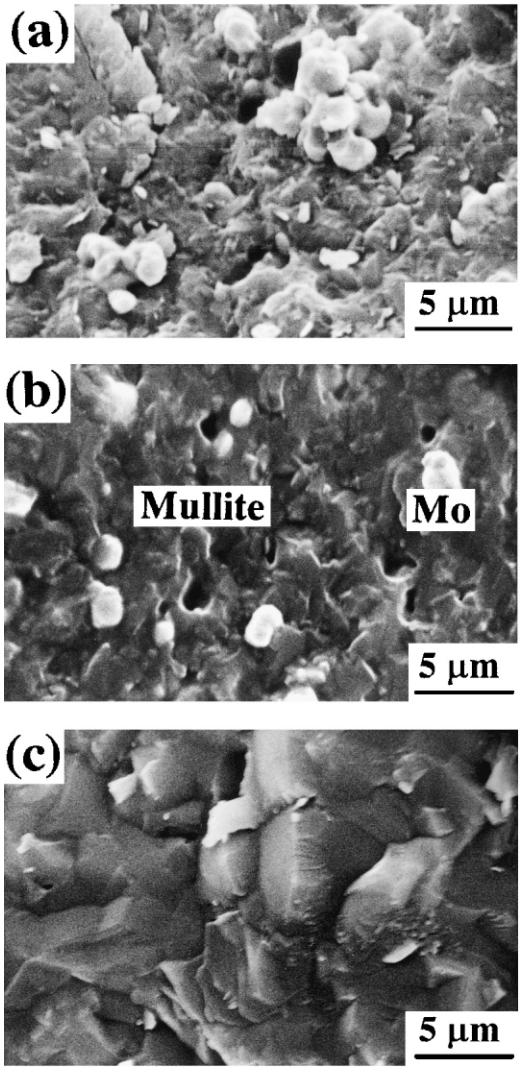

Fig. 3. Fractured surfaces of PECS sintered specimens. (a) 1090 N composite, (b) 1090 composite and (c) mullite.

The fracture strength and toughness simultaneously increased for the 1090 composite compared to the monolithic mullite. The bending strength of mullite increased significantly from 441 to 634 MPa, where 10 vol.% Mo and a small amount of MgO were incorporated in the matrix. The strengthening of the 1090 composite of mullite-Mo is mainly due to the smaller mullite grains, which is related to the reduction of the flaw size. Added MgO and molybdenum particles suppressed the grain growth of mullite. Reduced strength of the 1090 N composites is associated with agglomeration of Mo particles, relatively high porosity and elongated mullite morphology due to no addition of MgO.

The fracture toughness of the 1090 composites is nearly twice that of the monolithic mullite. Referring to the types of the toughening mechanisms mentioned above, the mechanisms of the 1090 composite may be due to the mechanism (A) of the frontal process-zone toughening mechanism and the mechanism (B) of the crack-bridging mechanism. Although the initial grain sizes of both mullite and Mo powder are slightly larger than 1 μm, the toughening mechanism of nanocomposites proposed by Niihara will be possibly expected in the 1090 composites, because the frontal process-zone size will be about 10 μm for structural ceramics [2]. As shown in Fig. 3, both of the composites 1090 and 1090 N indicate transgranular fracture and Mo particles are found on the fracture surface, which suggests that the Mo particles are mainly dispersed inside the mullite grains. However, the thermal expansion mismatch between the Mo and mullite is so small that nano-toughening mechanism will not operate enough in this case. In addition, the connection between the mullite matrix and Mo seems to be weak, because several holes after removing the Mo particles are observed on the fracture surface as shown in Fig. 3(b). Therefore, the ductile Mo particles may play a role of crack-bridging which increases an extrinsic fracture resistance of mechanism (B).

3.4. Thermal properties

Thermal properties of the monolithic mullite and mullite–Mo composites are given in Table 2. The thermal diffusivity is slightly higher for the composites than the mullite. This can be due to addition of Mo with high

Table 2
Thermal properties of mullite–Mo composites sintered by pulse electric current sintering, which were measured at room temperature

	Thermal diffusivity ($\times 10^{-6} m^2/s$)	Specific heat (J/kg/K)	Thermal conductivity (W/m/K)
1090N	2.5±0.3	660±8	5.9±0.8
1090	2.6±0.02	710±75	6.9±0.8
Mullite	2.4±0.05	930±3	6.9±0.05

thermal diffusivity (63×10^{-6} m^2/s) to the mullite. The thermal conductivity of the 1090 N composite is low because of the high porosity. The 1090 composites has the same thermal conductivity as the value of the monolithic mullite. Mo particles with high thermal conductivity (138 $Wm^{-1}K^{-1}$) are not contributed to increase in thermal conductivity of the composites, because they are well dispersed and discontinuous in the mullite matrix.

4. Conclusions

The monolithic mullite and Mo particles reinforced mullite matrix composites were fabricated using the PECS method. Dense samples obtained were more than 97% of the theoretical density under the sintering condition of 1500°C for 10 min. MgO has influence on the microstructural control and thus improved the mechanical and thermal properties of the mullite–Mo composites. Uniform dispersion of Mo particles in a mullite matrix having no agglomerations showed high fracture strength and toughness values by adding MgO. Strength of the 1090 composites increased to 634 MPa from 441 MPa for monolithic mullite due to smaller mullite grain size with reduced critical flaw size. For the 1090 N composites, the elongated mullite grains and agglomerate of Mo particles were found, which is mainly due to absence of MgO. Thus, the fracture strength and toughness for 1090 N composites were inferior to the 1090 composites. The elongation of mullite particles prevented by MgO addition promoted the sintering. Mo particles in mullite matrix could have pinned to control the microstructure of the 1090 composites, and resulted in improving the mechanical properties. The toughening mechanisms of mullite–Mo composites are mainly based on crack-bridging and nano-toughening, and the toughness increased twice that of the monolithic mullite. The slight increase of thermal diffusivity of the 1090 composites was obtained due to addition of Mo particles.

References

[1] K. Niihara, New design concept of structural ceramics — ceramic nanocomposites, J. Ceram. Soc. Japan 99 (10) (1991) 974–982.
[2] H. Awaji, S-M. Choi, T. Ebisudani, D.D. Jayaseelan, Toughening mechanisms of structural ceramics (in Japanese), J. Ceram. Soc. Japan 108 (6) (2000) 611–613.
[3] O. Sbaizero, G. Pezzotti, T. Nishida, Fracture energy and R-curve behaviour of Al_2O_3/Mo composites, Acta Mater. 46 (2) (1998) 681–687.
[4] H. Prielipp, M. Knechtel, N. Claussen, S.K. Streiffer, H. Mullejans, M. Ruhle, J. Ruhle, Strength and fracture toughness of aluminium/alumina composites with interpenetrating networks, Mater. Sci. Eng. A 197 (1995) 19–30.
[5] G.M. Song, Y. Zhou, Y. Sun, T.C. Lei, Computer simulation of crack propagation in whisker-reinforced ceramic composites, Ceram. Int. 24 (1998) 455–460.
[6] G. Pezzotti, H. Okuda, N. Muraki, T. Nishida, In-situ determination of bridging stresses in Al_2O_3-platelet composites by fluorescence spectroscopy, J. Eur. Ceram. Soc. 19 (1999) 601–608.
[7] W.J. Clegg, K. Kendall, N.McN Alford, T.W. Button, J.D. Birchall, A simple way to make tough ceramics, Nature 347 (1990) 455–457.
[8] W.J. Clegg, The fabrication and failure of laminar ceramic composites, Acta Metall. Mater. 40 (11) (1992) 3085–3093.
[9] H. Liu, S.M. Hsu, Fracture behaviour of multilayer silicon nitride/boron nitride ceramics, J. Am. Ceram. Soc. 79 (9) (1996) 2452–2457.
[10] D. Kovar, M.D. Thouless, J.W. Halloran, Crack deflection and propagation in layered silicon nitride/boron nitride ceramics, J. Am. Ceram. Soc. 81 (4) (1998) 1004–1012.
[11] Y. Shigegaki, M.E. Brito, K. Hirao, M. Toriyama, S. Kanzaki, Processing of a novel multilayered silicon nitride, J. Am. Ceram. Soc. 79 (8) (1996) 2197–2200.
[12] E.N. Drewry, R.J. Moon, K.J. Bowman, K.P. Trumble, Fracture behaviour of centrifugally cast multilayer alumina/alumina composites, Scripta Mater. 41 (7) (1999) 749–754.
[13] K. Hirao, M. Ohashi, M.E. Brito, S. Kanzaki, Processing strategy for producing highly anisotropic silicon nitride, J. Am. Ceram. Soc. 78 (6) (1995) 1687–1690.
[14] D. Doni Jayaseelan, S. Honda, T. Nishikawa, H. Awaji, Fabrication and characterization of mullite–Mo composites by pulse electric current sintering (PECS) technique, in: Proceedings of 16th Japan–Korea International Ceramics Seminar, Japan, 1999, pp. 88–92.
[15] D. Amutharani, D. Doni Jayaseelan, T. Nishikawa, H. Awaji, Pressureless sintering of mullite–Mo composites, J. Ceram. Soc. Japan (submitted for publication).
[16] R. Sivakumar, H. Takenaka, S. Honda, T. Nishikawa, H. Awaji, Temperature distributions in a stress relief type hollow cylinder of functionally graded materials under thermal shock, in: Proceedings of 16th Japan–Korea International Ceramics Seminar, Japan, 1999, pp. 324–328.
[17] R. Torrecillas, A.N. Espino, J.F. Bartolome, J.S. Moya, Functionally graded zircon–molybdenum materials without residual stresses, J. Am. Ceram. Soc. 83 (2) (2000) 454–456.
[18] L. Montanaro, C. Perrot, C. Esnouf, G. Thollet, G. Fantozzi, A. Negro, Sintering of industrial mullites in the presence of magnesia as a sintering aid, J. Am. Ceram. Soc. 83 (1) (2000) 189–196.
[19] Z.Y. Deng, J.L. Shi, Y.F. Zhang, D.Y. Jiang, J.K. Guo, Pinning effect of SiC particles on mechanical properties of Al_2O_3–SiC ceramic matrix composites, J. Eur. Ceram. Soc. 18 (1998) 501–508.
[20] W.H. Zhu, J.H. Gao, Z.S. Ding, Microstructure and mechanical properties of a Si_3N_4/Al_2O_3 nanocomposite, J. Mater. Sci. 32 (1997) 537–542.